

APPROVAL


**DETERMINATION OF THE HARDNESS DISTRIBUTION PATTERN
OBTAINED BY NITRIDING WITH A PLASMA FOCUS DEVICE**

by

Ng Chee An

A project dissertation submitted to the
Faculty of Engineering and Quantity Surveying
INTI INTERNATIONAL UNIVERSITY
in partial fulfilment of the requirement for the
Bachelor of Engineering (Hons) in
Mechanical Engineering

Approved:



Mr. Teh Thiam Oun
Project Supervisor

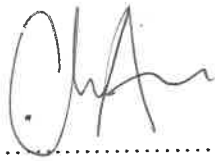
INTI INTERNATIONAL UNIVERSITY
NILAI, NEGERI SEMBILAN

April 2017

DECLARATION

I, the undersigned, hereby declare that this report is my own independent work except as specified in the references and acknowledgements. I have not committed plagiarism in the accomplishment of this work, nor have I falsified and/or invented the data in my work. I am aware of the University regulations on Plagiarism. I accept the academic penalties that may be imposed for any violation.

Signature



Name

NG CHEE AN

Matrix No.

I 13003611

Date

12 JULY 2017

ABSTRACT

Plasma focus nitriding is one of the case-hardening method which utilizes energetic bombardment of nitrogen ion beam, produced through high temperature due to electrical discharge at high voltage, onto the target material surface. Experiment was carried out by nitriding low carbon steel samples AISI 1020 using different combination of nitrogen pressure (0.5 Torr, 1.0 Torr, 1.5 Torr, 2.0 Torr) and sample distance from anode tip (40 mm, 60 mm, 80 mm, 100 mm, 120 mm), by using UNU/ICTP PFF plasma focus device which was charged initially at 12 kV. Each sample was fired by 30 shots of nitrogen ion beam. The result showed that the plasma focus nitriding produced a localized hardening region near the epicentre of plasma pinch, with diameter ranged between 15 mm – 30 mm. The maximum Vickers microhardness measured was 429.1 HV 0.2, at nitrogen pressure of 1.0 Torr and distance from anode of 40 mm. Layering ring-like pattern was observed on the nitrided steel surface. Samples closer to the anode tip (40 mm to 60 mm) exhibited localized rough surface near epicentre, which coincided with the localized hardening region. Radiative Dense Plasma Focus Computation Package (RADPF) software – Lee model code was implemented to generate nitrogen beam related parameters using differential current waveform obtained experimentally. Model fitting and numerical simulation result showed that the optimum plasma focusing in nitrogen environment took place at around 1.0 Torr – 1.5 Torr,

DEDICATION

This thesis is dedicated to my parents, Ng Boon Shyong & Tan Geok Kiow.

TABLE OF CONTENTS

DECLARATION	i
ABSTRACT	ii
ACKNOWLEDGEMENTS	iii
DEDICATION	iv
LIST OF FIGURES	vii
LIST OF TABLES	ix
LIST OF ABBREVIATIONS	x
NOMENCLATURE	xi
CHAPTER 1 INTRODUCTION	1
1.1. Background	1
1.2. Problem Statements	2
1.3. Objectives of the Research	2
1.4. Scope of the Research	3
1.5. Report Organization	3
CHAPTER 2 LITERATURE REVIEW	5
2.1. Definition of Plasma	5
2.1.1. Degree of Ionization	6
2.1.2. Quasi-neutrality of Plasma	7
2.1.3. Velocity Distribution, Ion Temperature and Electron Temperature	7
2.2. Operation of Dense Plasma Focus Device	8
2.2.1. Plasma Instabilities	10
2.2.2. Optimization of DPF Device	13
2.2.3. Phenomenon of Sputtering	14
2.2.4. Types of Deposition Films	15
2.2.5. Working Principle of Rogowski Coil	16
2.3. Material Properties of AISI 1020 Low Carbon Steel	18
2.3.1. Heat Treatment of Steels	18

2.4. Vickers Microhardness Testing	21
CHAPTER 3 EXPERIMENTAL METHODOLOGY	24
3.1. Sample Preparation	24
3.2. Plasma Treatment of AISI 1020 Steel Samples	31
3.3. Current Model Fitting and Numerical Simulation Using Lee Model Code	37
CHAPTER 4 EXPERIMENTAL RESULTS	42
4.1. Hardness Distribution Comparison between Nitrided and Unnitrided Steel	42
4.2. Layering Pattern on Nitrided Steel Surface	54
4.3. Correlation between Layering Pattern and Hardness Distribution	63
4.4. Ion Beam Analysis Using Lee Model Code	64
4.5. Correlation between Ion Beam Parameters and Hardening Effect	66
CHAPTER 5 CONCLUSION	67
5.1. Summarization of Project	67
5.2. Recommendation	68
5.3. Future Work	68
REFERENCES	69
Appendix A Project Gantt Chart	72
Appendix B Vickers Microhardness Test Result (First Trial)	73
Appendix C Vickers Microhardness Test Result	76
Appendix D Fitted Model Parameters	120

LIST OF FIGURES

Figure 1: The Schematic of DPF Material Processing.....	9
Figure 2: Operation Stages of Dense Plasma Focus Device.....	9
Figure 3: Sausage Instability.....	11
Figure 4: Kink Instability.....	12
Figure 5: Formation of sausage instabilities in plasma column with oval anode.	12
Figure 6: The Presence of Voltage Spike and Current Dip in The Waveform	13
Figure 7: Schematic Illustration of Physical Sputtering Process.....	14
Figure 8: Structure of Rogowski Coil.....	17
Figure 9: The Fe – Fe ₃ C phase diagram (Dossett & Boyer, 2006).....	19
Figure 10: The effect of carbon and heat treatment on the properties of plain carbon steel	20
Figure 11: Diamond Shape Indenter and Diagonal Lengths in Vickers Hardness Test	22
Figure 12: Planned Overall Sample Preparation Process Flow	24
Figure 13: Dimensions for Band Saw Cutting (75mm x 30mm).....	25
Figure 14: Mastika Metal Horizontal Band Saw	25
Figure 15: Detailed View of Band Saw Cutting	26
Figure 16: Steel Samples Milling	26
Figure 17: Nabertherm Chamber Furnace for Annealing Process.....	27
Figure 18: Heating Temperature in Variation with Time During Annealing Process.....	27
Figure 19: Detailed Surface Grinding Process with Different Grit Sizes.....	28
Figure 20: Vickers Hardness Measuring Points.....	29
Figure 21: Heating Temperature in Variation with Time During Improved Annealing Process	30
Figure 22: Vickers Hardness Result of Untreated AISI 1020 Steel Samples	30
Figure 23: INTI IU Mather-Type 3 kJ DPF Device	31
Figure 24: General Process Flow of Plasma Firing	32
Figure 25: Cleaning of AISI 1020 Steel Samples Using Propan-2-ol	33
Figure 26: Marking of Distance of Sample from The Top of Anode	33
Figure 27: Franklin Electric Vacuum Pump for DPF Cavity Evacuation	34
Figure 28: Pressure Gauge Indicating DPF Cavity Pressure Close to Zero	34

Figure 29: Waveform Responses During Test Plasma Shot.....	35
Figure 30: Voltage Spike During the Formation of Plasma Pinch	36
Figure 31: CSV File Containing Electrical Waveform Data	38
Figure 32: Experimental Current Waveform Displayed in Lee Model Code.....	39
Figure 33: Parameters Required In Lee Model Code	39
Figure 34: Model Fitting Result Using Lee Model Code	40
Figure 35: Computed Ion Beam Parameters Displayed in Lee Model Code.....	41
Figure 36: Hardness Distribution of Nitrided and Unnitrided Sample S1.....	43
Figure 37: Hardness Distribution of Nitrided and Unnitrided Sample S2.....	43
Figure 38: Hardness Distribution of Nitrided and Unnitrided Sample S3.....	44
Figure 39: Hardness Distribution of Nitrided and Unnitrided Sample S4.....	44
Figure 40: Hardness Distribution of Nitrided and Unnitrided Sample S5.....	45
Figure 41: Hardness Distribution of Nitrided and Unnitrided Sample S6.....	45
Figure 42: Hardness Distribution of Nitrided and Unnitrided Sample S7.....	46
Figure 43: Hardness Distribution of Nitrided and Unnitrided Sample S8.....	46
Figure 44: Hardness Distribution of Nitrided and Unnitrided Sample S9.....	47
Figure 45: Hardness Distribution of Nitrided and Unnitrided Sample S10.....	47
Figure 46: Hardness Distribution of Nitrided and Unnitrided Sample S11.....	48
Figure 47: Hardness Distribution of Nitrided and Unnitrided Sample S12.....	48
Figure 48: Hardness Distribution of Nitrided and Unnitrided Sample S13.....	49
Figure 49: Hardness Distribution of Nitrided and Unnitrided Sample S14.....	49
Figure 50: Hardness Distribution of Nitrided and Unnitrided Sample S15.....	50
Figure 51: Hardness Distribution of Nitrided and Unnitrided Sample S16.....	50
Figure 52: Hardness Distribution of Nitrided and Unnitrided Sample S17.....	51
Figure 53: Hardness Distribution of Nitrided and Unnitrided Sample S18.....	51
Figure 54: Hardness Distribution of Nitrided and Unnitrided Sample S19.....	52
Figure 55: Hardness Distribution of Nitrided and Unnitrided Sample S20.....	52
Figure 56: EDX Result on Nitrided Steel using UNU/ICTP PFF (30 shots).....	58
Figure 57: Vickers Microhardness Colour Mapping	62
Figure 58: 20x Microscopic View of Sample 6 (40 mm, 1 Torr) Surface.....	63

LIST OF TABLES

Table 1: Detailed Operations Involved in Various Stages of Plasma Focusing	10
Table 2: Mechanical Properties and Major Applications of Several Deposition Film Materials.	15
Table 3: Compositions of AISI 1020 Steel (AZo Materials, 2012).....	18
Table 4: Operating Conditions of Different Steel Samples	37
Table 5: Machine and Operational Parameters Used in Lee Model Code.....	40
Table 6: Maximum Measured Vickers Microhardness of Nitrided Steel Samples	54
Table 7: Ring Pattern on Nitrided AISI 1020 Steel Surfaces (Units in mm).....	55
Table 8: Layering Pattern of Nitrided Steel at 0.5 Torr Nitrogen Pressure	56
Table 9: Layering Pattern of Nitrided Steel at 1.0 Torr Nitrogen Pressure	58
Table 10: Layering Pattern of Nitrided Steel at 1.5 Torr Nitrogen Pressure	59
Table 11: Layering Pattern of Nitrided Steel at 2.0 Torr Nitrogen Pressure	60
Table 12: Correlation Between Hardening Region and Ring Pattern on Nitrided Steel	63
Table 13: Ion Beam Parameters Obtained from Lee Model Code Simulation for Every Nitrided Steel Sample	64
Table 14: Average Ion Beam Parameters Obtained from Lee Model Code Simulation for Each Nitrogen Pressure	65
Table 15: Correlation between Average Number of Ions per Shot and Vickers Microhardness At Different Nitrogen Pressures	66

LIST OF ABBREVIATIONS

DPF	Dense Plasma Focus
RADPF	Radiative Dense Plasma Focus
MHD	Magnetohydrodynamics
AC	Alternating Current

NOMENCLATURE

<i>Symbol</i>	<i>Definition</i>
h	Planck's constant (6.63×10^{-34} J s)
ν	Frequency of photon [Hz]
n_i	Density of ionized atoms [m^{-3}]
n_n	Density of neutral atoms [m^{-3}]
T	Gas temperature [K]
k	Boltzmann's constant (1.38×10^{-23} J K ⁻¹)
U_i	Ionization energy of gas [J]
n_e	Electron density [m^{-3}]
n_z	Z-times charged ion density [m^{-3}]
E_{av}	Average kinetic energy [J]
f	Degree of freedom of gas molecule
E	Electric field [N C^{-1}]
k	Coulomb's constant (9.0×10^9 N m ² C ⁻²)
Q, q	Electrical charge [C]
r	Distance length [m]
F	Coulomb force [N]
p	Kinetic pressure of plasma [Pa]
p_{m0}	Magnetic pressure at plasma surface [Pa]
B_0	Magnetic flux density at plasma surface [T]
μ_0	Vacuum permeability ($4\pi \times 10^{-7}$ T m A ⁻¹)
I, i	Current [A]
A	Cross-sectional area of Rogowski coil [m ²]
n	Number of turns per unit circumferential length [m ⁻¹]
$d_{1,2}$	Diagonal length of Vickers indentation [mm]
d	Arithmetic mean of diagonal lengths [mm]
F	Indentation test force [N]
HV	Vickers hardness
α	Angle between opposite faces of pyramidal indenter

CHAPTER 1

INTRODUCTION

1.1. Background

In the daily operation of complicated machines, there is one factor that is difficult to be eliminated and unavoidably causes failure in machines – friction. Friction may come into serious negative effects like surface wearing when improper or lack of lubrication is implemented. In order to improve the wear resistance of machine parts without affecting the interior bulk material properties of the parts, a process called “surface hardening” is introduced and applied by means of a wide variety of mechanisms.

Surface hardening process is very useful in machinery parts such as cams, bearings, shafts, turbine applications and automotive components. These types of machinery parts require high surface hardness to resist wearing, while maintaining tough interior strength to withstand forces applied when the relevant machines are operating (Dossett & Totten, 2013).

Surface hardening has a wide engineering application in several practical aspects, such as the safety concerns in building or bridge construction, machineries components. Mechanical wear may be accelerated by chemical damage to the worn materials. The collapse of Mianus River Bridge in Greenwich, Connecticut, USA in 1983 was one of the disastrous tragedies in engineering history due to the reason of metal corrosion and wearing. This tragedy caused four people killed and five people injured during the collapse (Ben-Daya, Kumar, & Prabhakar, 2016). Similar engineering tragedies has introduced the highlights and considerations of issues in mechanical wearing and surface hardness as one of the factors to ensure that the structural design is successful and has no potential safety hazards to relevant people.

Dense plasma focus device (PDF) is an unconventional plasma device which has the capability of producing X-rays, neutrons, relativistic electrons and energetic ion beams. These are essentially very useful in some applications, for example surface treatment,

thin layer deposition, sputtering and modification of materials. By mean of implementing the dense plasma focus device, the surface material properties of the target specimen like hardness, corrosion and wear resistances can be altered and controlled through surface coating process (Al-Hawat, Soukieh, Kharoub, & Al-Sadat, 2010).

1.2. Problem Statements

The dominant concern in the surface coating process of dense plasma focus device is that, the surface hardening effect is not the same at various distances from epicentre. The effectiveness of hardness improvement is varying at different surface locations on the coated specimen. There may be cases when the hardness near the epicentre is sufficient, but the hardness at a further distance away is below specification.

Due to this reason, it is required to understand the relationship between the surface strengthening effect and the distance to plasma shot epicentre, to ensure that the surface hardness of the coated surface can withstand the forces exerted onto the surface at all times without resulting in surface wearing.

In order to carry out investigation for this Final Year Project, a Mather-type 3 kJ DPF device was implemented to perform the plasma treatment on the target AISI 1020 low carbon steel samples.

1.3. Objectives of the Research

The overall objectives of the research can be as follows:

- To investigate and develop the hardness distribution pattern of nitriding using Mather-type 3 kJ DPF device (UNU/ICTP PFF) through experiments.
- To analyse and identify the relevant factors affecting the hardness distribution pattern.
- To determine the optimum condition of plasma focusing in nitrogen-filled environment experimentally and numerically.

1.4. Scope of the Research

In Final Year Project Stage 1, due to the limitations of time constraints raised from the open timeslots of workshop and material laboratory, AISI 1020 steel material samples preparation such as material bar cutting, milling, grinding, hardness measuring and literature review research were more focused in this stage.

The Stage 2 was more focused on the experimental nitriding process by using UNU/ICTP PFF device, and analysis of the experimental results to study the effect of distance from the epicentre of the target on the amount of hardening in a PF device. Radiative Dense Plasma Focus Computation Package (RADPF) a.k.a. Lee model code was also implemented to perform computational simulations for the correlation with experimental results. The effect of surface hardening was correlated to the number of ions produced during plasma nitriding, which values were obtained through current model fitting and computational simulation using Lee model code.

1.5. Report Organization

This Final Year Project Interim Report covers the following aspects:

- Chapter 2: Literature Review
 - Characteristics and properties of fourth state of matter – plasma.
 - Operation of Dense Plasma Focus (DPF) device.
 - Related mechanical properties of AISI 1020 low carbon steel required for samples preparation.
 - Method of Vickers hardness testing, as of ISO 6507-1:2005 required.
- Chapter 3: Methodology
 - Method to fabricate required steel samples.
 - Parameters and dimensional decisions of certain processes.
 - Procedures of operating DPF device.
 - Implementation of Lee model code for numerical simulation of plasma pinching process.
- Chapter 4: Experimental Results
 - Hardness distribution comparison between nitrided and unnitrided steel.

- Layering pattern appearance on nitrided steel surface.
- Correlation between hardening region and layering pattern.
- Numerical ion beam analysis using Lee model code.
- Correlation between experimental and numerical results.
- Chapter 5: Conclusion
 - Summarization of overall project.
 - Relation between plasma nitriding and real life engineering application.
 - Recommendation on related project.
 - Possible future work ahead.